5-1-1993

Spontaneous coherent pulsations in standing-wave laser oscillators: stability criteria for homogeneous broadening

Pitak Chenkosol
Portland State University

Lee W. Casperson
Portland State University

Citation Details

Pitak Chenkosol and Lee W. Casperson, "Spontaneous coherent pulsations in standing-wave laser oscillators: stability criteria for homogeneous broadening," J. Opt. Soc. Am. B 10, 817-826 (1993).

Spontaneous coherent pulsations in standing-wave laser oscillators: stability criteria for homogeneous broadening

Pitak Chenkosol and Lee W. Casperson

Department of Electrical Engineering, Portland State University, P.O. Box 751, Portland, Oregon 97207-0751

Received July 15, 1992; revised manuscript received October 7, 1992

The stability criteria for single-mode standing-wave laser oscillators in the homogeneously broadened limit are reported, and two types of criteria are distinguished. The first type (type 1) corresponds to the minimum value of the threshold parameter for which an infinitesimal perturbation away from steady state grows into an oscillatory solution. A second type (type 2) corresponds to the minimum value of threshold parameter for which large-amplitude oscillations do not decay to the steady-state solution. Undamped pulsations in single-mode homogeneously broadened standing-wave laser oscillators are found to occur at a much higher excitation level than in ring-laser oscillators with homogeneous broadening. The effects of detuning on the stability criteria are also investigated.

1. INTRODUCTION

Instabilities and nonlinear dynamics of lasers are of great theoretical and experimental interest, and this subject has been reviewed in many publications.[1-8] Most of the effort relating to laser instabilities has focused on ring-laser systems in which the electromagnetic fields are understood to propagate in one direction through the laser amplifier. To observe semiclassical spontaneous pulsation behavior in a homogeneously broadened ring-laser system, one must operate the laser at an excitation level at least nine times above the lasing threshold and also satisfy the condition that the decay rate of the cavity fields be higher than the sum of the decay rates of the polarization and inversion. In the line center tuned case, the equations governing a single-mode homogeneously broadened ring laser have the same form as the equations of the Lorenz model governing a low-dimensional hydrodynamic system.[9,10] Much effort has been spent in trying to observe experimentally this Lorenz instability, which has been known in various forms since soon after the first laser was built. The simultaneous requirements of a large field decay rate and a large threshold parameter make this instability unlikely to occur in practical laser systems. Recently, however, its possible observation has been reported.[11-19] In contrast to homogeneously broadened lasers, inhomogeneously broadend lasers possess a low threshold instability. Semiclassical spontaneous pulsation behavior was first observed in inhomogeneously broadened xenon lasers,[20,21] and current theoretical models for that system provide good agreement with experimental observations.

Thus far, there is no experimental proof for the existence of the Lorenz instability in practical laser systems, although Lorenz-like signals have been reported recently in experiments with optically pumped far-infrared ammonia ring lasers.[18,19] These lasers are basically described by a three-level model in which coherent pumping effects may play a significant role in the dynamic behavior. The Lorenz model, on the other hand, assumes an incoherently pumped two-level model. Under certain restrictive conditions of lifetimes and pump rates, however, the theoretical model for three-level far-infrared ring lasers may be simplified to the two-level Lorenz model.[22] It has also been suggested that Doppler broadening, which was not included in earlier studies, may reduce the coherent effects of the optical pumping and lead to better qualitative agreement with the Lorenz model.[23]

In many experiments with ammonia lasers, the intensity of the laser output is the fundamental quantity measured.[12-15,24] The spiral-type intensity patterns have been emphasized because they are characteristic of the Lorenz attractor, and there are reports of Lorenz-like signals from these lasers. However, these observations alone are not sufficient to prove that the attractor is of the true symmetric Lorenz type.[18] This difficulty has led to a search for some other quantities to measure that might help to identify real Lorenz signals. Heterodyne measurements of the field amplitudes and phases of the laser signal have been performed in addition to the intensity measurements,[25-30] and theoretical studies of this subject can be found in Refs. 31 and 32. References 23 and 28 show that the field amplitude may be constant in sign in the Lorenz-like cases but alternates in sign in the true Lorenz model. Additionally, the phase plot measurements of Lorenz-like cases may show asymmetric patterns in phase space in contrast to the symmetric patterns of the Lorenz model. The phase measurement patterns also reveal the presence or absence of phase jumps by π rad, which indicates changes in sign of the field amplitude between successive spirals, as predicted by the Lorenz model.[25,27,28,31]

Qualitative agreement between the dynamics of the complex Lorenz equations and experimental data for a detuned ammonia laser were reported in Refs. 29 and 30. Also, at high gas pressure (above 10 Pa) the dynamic evolution of the ammonia far-infrared ring lasers shows a closer similarity to the Lorenz model than at lower pressure.[7,15,23,25,26,29] Several statistical dynamic properties have also been investigated, including cusp-map, spiral-length, and pulse-height distributions.[18,19,33] Recently the presence of a counterpropagating signal field was also shown to affect the intensity spiral dynamics.[19] Under

0740-3224/93/050817-10$05.00

certain operating conditions, where this counterpropagating signal field is absent, Lorenz-like spiral intensity signals were observed. To date, none of the reported experiments has shown the large difference between the perturbation and large signal instability thresholds known to exist in the Lorenz model.[34]

To summarize the ring-laser work, the results of experiments performed on ammonia far-infrared lasers have provided good qualitative agreement with many features of the Lorenz model. However, it is usually acknowledged that the resulting signals are only Lorenz-like rather than indicators of a true Lorenz attractor. Nevertheless, efforts to find the Lorenz attractor in lasers seems to be continuing, and it may be possible to choose conditions in far-infrared lasers in which significant deviations from the Lorenz dynamics are absent.[19]

The majority of studies dealing with laser instabilities has focused on one-directional ring lasers, as discussed above. These systems tend to be easier to analyze than bidirectional or standing-wave lasers, because in one-directional ring lasers the rapid time and space dependences of the field, polarization, and population parameters can be factored out of the theoretical model. However, standing-wave lasers are more common in practice. For example, the xenon laser with which the semiclassical instabilities were first studied was a standing-wave device. Thus important reasons exist for investigating the instability characteristics of standing-wave lasers. General theoretical models have been developed to interpret the standing-wave xenon laser data, and good agreement with the experimental data has been obtained.[35] The complexities of the laser equations usually prevent one from solving them analytically, although some analytical results can be obtained. Numerical solutions, however, are always possible, and such solutions have been most useful in studies of the xenon laser. The main difficulty with numerical solutions is that they require substantial computing resources and are costly to carry out. Any results obtained will not be applicable to other laser systems, because different systems would be characterized by different sets of operating parameters. Therefore it would be useful to develop some graphical representations of the instability behavior that could be applied to broad classes of lasers. The stability criteria are extremely useful representations of this type.

Stability criteria are curves that show the ranges of parameters for which a laser will produce stable continuous-wave output and the ranges for which the output will consist of pulsations. Because only a limited number of parameter variations can be represented on a graph, the laser equations must be simplified first. The resulting instability boundaries can be used to test qualitatively whether a given continuously pumped laser will produce its output in the form of undamped pulsations. These results are useful for estimating the behavior of a laser under study, even if they do not provide direct information regarding the pulsation waveforms. If necessary, the actual waveforms can always be obtained by direct numerical integration of the dynamic equations governing the behavior of the laser system.

In this study we emphasize two types of stability criteria that are associated with the nontrivial steady-state solutions of the laser equations. The first criterion, which we call type 1, corresponds to the minimum value of the threshold parameter for which an infinitesimal perturbation away from the steady-state solution grows into an undamped oscillatory solution. The other criterion, which we call type 2, corresponds to the minimum value of the threshold parameter for which large-amplitude oscillatory solutions do not decay to the steady-state solution. As noted previously, the stability of the steady-state solution depends on the magnitude of the perturbations to which it is subjected.[34] A large perturbation may cause the onset of pulsations, whereas a small perturbation may not. For ring lasers, a large range of these stability criteria were described previously for line broadening ranging from the homogeneous to the inhomogeneous limit and including the effects of detuning from line center.[34–37] The main purpose of this study is to develop the same kinds of stability criteria for standing-wave lasers. Although the initial analysis here is general, the emphasis is on homogeneously broadened lasers. The most striking feature of the results is that the minimum value of the excitation level needed for homogeneously broadened standing-wave lasers to produce their output in the form of undamped pulsations is much higher than that for ring lasers. In other words, in the homogeneous broadening limit standing-wave lasers are much more stable than ring lasers.

The basic dynamic equations governing the semiclassical instability of standing-wave lasers are reviewed and simplified in Section 2. In Section 3 the model is expanded into a larger set describing the various spatial harmonics of the standing-wave fields, polarizations, and populations. A linear stability analysis for determining the type 1 or perturbation stability boundaries for homogeneously broadened lasers is introduced in Section 4. The resulting stability boundaries are presented in a series of graphs in Section 5, and the effects of detuning from line center are also described.

2. THEORY

The model underlying our stability analysis is based on the semiclassical Maxwell–Schrödinger equations for a laser oscillator. In various forms this model has been the basis for most semiclassical laser studies since the early work of Lamb,[38] but other equivalent starting formulations are also possible.[39] We will begin with a generalized set of Lamb equations in the form[40]

$$\left(\frac{\partial}{\partial t}+v\frac{\partial}{\partial z}\right)P_r(v,\omega_\alpha,z,t)=-(\omega-\omega_\alpha)P_i(v,\omega_\alpha,z,t)-\gamma P_r(v,\omega_\alpha,z,t)+\frac{\mu^2}{\hbar}\sin(kz)E_i(t)D(v,\omega_\alpha,z,t), \tag{1}$$

$$\left(\frac{\partial}{\partial t}+v\frac{\partial}{\partial z}\right)P_i(v,\omega_\alpha,z,t)=(\omega-\omega_\alpha)P_r(v,\omega_\alpha,z,t)-\gamma P_i(v,\omega_\alpha,z,t)-\frac{\mu^2}{\hbar}\sin(kz)E_r(t)D(v,\omega_\alpha,z,t), \tag{2}$$

$$\left(\frac{\partial}{\partial t} + v\frac{\partial}{\partial z}\right)D(v,\omega_\alpha,z,t) = \lambda_a(v,\omega_\alpha,z,t) - \lambda_b(v,\omega_\alpha,z,t) - \frac{\gamma_a + \gamma_{ab} + \gamma_b}{2}D(v,\omega_\alpha,z,t) - \frac{\gamma_a + \gamma_{ab} - \gamma_b}{2}M(v,\omega_\alpha,z,t) + \frac{\sin(kz)}{\hbar}[E_r(t)P_i(v,\omega_\alpha,z\,t) - E_i(t)P_r(v,\omega_\alpha,z,t)], \quad (3)$$

$$\left(\frac{\partial}{\partial t} + v\frac{\partial}{\partial z}\right)M(v,\omega_\alpha,z,t) = \lambda_a(v,\omega_\alpha,z,t) + \lambda_b(v,\omega_\alpha,z,t) - \frac{\gamma_a - \gamma_{ab} - \gamma_b}{2}D(v,\omega_\alpha,z,t) - \frac{\gamma_a - \gamma_{ab} + \gamma_b}{2}M(v,\omega_\alpha,z,t), \quad (4)$$

$$\frac{dE_r(t)}{dt} = -\frac{E_r(t)}{2t_c} - (\omega - \Omega)E_i(t) - \frac{\omega_0}{\epsilon_1 L}\int_0^\infty\int_{-\infty}^\infty\int_0^l \sin(kz)P_i(v,\omega_\alpha,z,t)dz\,dv\,d\omega_\alpha, \quad (5)$$

$$\frac{dE_i(t)}{dt} = -\frac{E_i(t)}{2t_c} + (\omega - \Omega)E_r(t) + \frac{\omega_0}{\epsilon_1 L}\int_0^\infty\int_{-\infty}^\infty\int_0^l \sin(kz)P_r(v,\omega_\alpha,z,t)dz\,dv\,d\omega_\alpha, \quad (6)$$

where the subscripts a and b denote the upper and lower laser levels, respectively; γ_a and γ_b are the total decay rates from these levels; γ_{ab} is the rate of direct decays from level a to level b, γ is the decay rate for the off-diagonal density matrix elements; λ_a and λ_b are the pumping rates; ω_α is the center frequency of the laser transition for members of an atomic or molecular class α; μ is the dipole moment for the laser transition; ω would be the actual radian frequency of the electromagnetic wave if the complex field amplitude were independent of time t; Ω is the nondispersed lasing frequency; ω_0 is a characteristic center frequency for the transition, l is the length of the laser amplifier; L is the mirror spacing; ϵ_1 is the background permittivity; t_c is the cavity lifetime; and the c.c. means the complex conjugate of the preceding terms. The dependent variables $P_r(v,\omega_\alpha,z,t)$ and $P_i(v,\omega_\alpha,z,t)$ are the real and imaginary parts, respectively, of the complex polarization $P'(v,\omega_\alpha,z,t)$; and $E_r(t)$ and $E_i(t)$ are the real and imaginary parts of the complex electric field $E'(t)$. These complex amplitudes are in turn related to the off-diagonal matrix element and the real electric field by the equations

$$\rho_{ab}(v,\omega_\alpha,z,t) = P'(v,\omega_\alpha,z,t)\exp(-i\omega t)/2\mu, \quad (7)$$

$$E(z,t) = \tfrac{1}{2}\sin(kz)E'(t)\exp(-i\omega t) + \text{c.c.}, \quad (8)$$

where the $\sin(kz)$ factor represents the assumed sinusoidal spatial dependence of the electric field. The population difference and sum in Eqs. (1)–(4) are related to the diagonal elements of the density matrix by the equations

$$D(v,\omega_\alpha,z,t) = \rho_{aa}(v,\omega_\alpha,z,t) - \rho_{bb}(v,\omega_\alpha,z,t), \quad (9)$$

$$M(v,\omega_\alpha,z,t) = \rho_{aa}(v,\omega_\alpha,z,t) + \rho_{bb}(v,\omega_\alpha,z,t). \quad (10)$$

In this analysis the possibility of spectral cross relaxation is excluded at the outset.

Equations (1)–(6) are a complete set governing the evolution of the fields, polarizations, and populations in a standing-wave laser oscillator. In our study of laser instabilities, we have taken two different approaches to the study of these equations. In one approach we obtained numerical solutions of the equations, while in the other approach we carried out a semianalytical stability analysis of a simplified form of the equations. We describe here the formulation used in our numerical solutions, and the analytical procedure is discussed in Section 3.

Although it is possible to solve Eqs. (1)–(6) numerically in their present form, several possible reductions of these equations can make the solutions more efficient without loss of practical relevance. A detailed discussion of these reductions is included in Refs. 35 and 41, and only a brief sketch is given here. One particular difficulty with the above model is that it includes partial derivatives with respect to both the space and time variables. Because of the high spatial frequency of the fields in most lasers, it is efficient to decompose the polarization and population into a series of spatial harmonics of the electric field. Thus we have introduced the expansions

$$P_r(v,\omega_\alpha,z,t) = \sum_{j=-\infty}^{\infty} P_{r,2j+1}(v,\omega_\alpha,t)\exp[(2j+1)ikz], \quad (11)$$

$$P_i(v,\omega_\alpha,z,t) = \sum_{j=-\infty}^{\infty} P_{i,2j+1}(v,\omega_\alpha,t)\exp[(2j+1)ikz], \quad (12)$$

$$D(v,\omega_\alpha,z,t) = \sum_{j=-\infty}^{\infty} D_{2j}(v,\omega_\alpha,t)\exp[(2j)ikz], \quad (13)$$

$$M(v,\omega_\alpha,z,t) = \sum_{j=-\infty}^{\infty} M_{2j}(v,\omega_\alpha,t)\exp[(2j)ikz], \quad (14)$$

where only odd harmonics of the polarizations and even harmonics of the populations are included.

It is also helpful to introduce normalized forms of the various parameters that will permit the most compact expression of the laser equations, and we have adopted the following set[35]:

$$A_r(t) = \frac{\mu}{2\hbar}\left(\frac{\gamma_a - \gamma_{ab} + \gamma_b}{2\gamma\gamma_a\gamma_b}\right)^{1/2}E_r(t), \quad (15)$$

$$A_i(t) = \frac{\mu}{2\hbar}\left(\frac{\gamma_a - \gamma_{ab} + \gamma_b}{2\gamma\gamma_a\gamma_b}\right)^{1/2}E_i(t), \quad (16)$$

$$P_{i,j}(V,U,t) = \frac{\epsilon u\gamma t_c\omega_0 l\mu}{\epsilon_1 L\hbar}\left(\frac{\gamma_a - \gamma_{ab} + \gamma_b}{2\gamma\gamma_a\gamma_b}\right)^{1/2}P_{i,j}(v,\omega_\alpha,t), \quad (17)$$

$$P_{r,j}(V,U,t) = \frac{\epsilon u\gamma t_c\omega_0 l\mu}{\epsilon_1 L\hbar}\left(\frac{\gamma_a - \gamma_{ab} + \gamma_b}{2\gamma\gamma_a\gamma_b}\right)^{1/2}P_{r,j}(v,\omega_\alpha,t), \quad (18)$$

$$D_{2j}(V,U,t) = \frac{\epsilon u t_c\omega_0 l\mu^2}{\epsilon_1 L\hbar}D_{2j}(v,\omega_\alpha,t), \quad (19)$$

$$M_{2j}(V,U,t) = \frac{\epsilon u t_c\omega_0 l\mu^2}{\epsilon_1 L\hbar}M_{2j}(v,\omega_\alpha,t), \quad (20)$$

$$\lambda_a(V,U,t) = \frac{\epsilon u t_c \omega_0 l \mu^2}{\epsilon_1 L \hbar} \lambda_a(v,\omega_\alpha,t), \tag{21}$$

$$\lambda_b(V,U,t) = \frac{\epsilon u t_c \omega_0 l \mu^2}{\epsilon_1 L \hbar} \lambda_b(v,\omega_\alpha,t), \tag{22}$$

where we have introduced the new variables

$$V = \frac{v}{\epsilon u} = \frac{kv}{\gamma}, \tag{23}$$

$$U = \frac{\omega_\alpha - \omega_0}{\gamma}. \tag{24}$$

Other parameters appearing in these equations include the most probable speed of the atoms or molecules, u, and the natural damping ratio $\epsilon = (\Delta\nu_h/\Delta\nu_d)(\ln 2)^{1/2}$. It is also convenient to introduce the normalized lasing frequency $y = (\omega - \omega_0)/\gamma$, the normalized cavity frequency $y_0 = (\Omega - \omega_0)/\gamma$, the new decay rate $\gamma_1 = 2\gamma_a\gamma_b/(\gamma_a - \gamma_{ab} + \gamma_b)$, and the decay parameter $\delta = 2\gamma t_c$. When this notation is used, Eqs. (1)–(6) take the form

$$\frac{\partial P_{r,2j+1}(V,U,t)}{\partial t} = -\gamma\{[1 + (2j+1)iV]P_{r,2j+1}(V,U,t) + (y-U)P_{i,2j+1}(V,U,t) + iA_i(t) \times [D_{2j}(V,U,t) - D_{2j+2}(V,U,t)]\}, \tag{25}$$

$$\frac{\partial P_{i,2j+1}(V,U,t)}{\partial t} = -\gamma\{[1 + (2j+1)iV]P_{i,2j+1}(V,U,t) - (y-U)P_{r,2j+1}(V,U,t) - iA_r(t) \times [D_{2j}(V,U,t) - D_{2j+2}(V,U,t)]\}, \tag{26}$$

$$\frac{\partial D_{2j}(V,U,t)}{\partial t} = [\lambda_a(V,U,t) - \lambda_b(V,U,t)]\delta_{j0} - \left[\frac{\gamma_a + \gamma_{ab} + \gamma_b}{2} + (2j)i\gamma V\right]D_{2j}(V,U,t) - \frac{\gamma_a + \gamma_{ab} - \gamma_b}{2}M_{2j}(V,U,t) - i\gamma_1\{[A_r(t)P_{i,2j-1}(V,U,t) - A_i(t) \times P_{r,2j-1}(V,U,t)] - [A_r(t)P_{i,2j+1}(V,U,t) - A_i(t)P_{r,2j+1}(V,U,t)]\}, \tag{27}$$

$$\frac{\partial M_{2j}(V,U,t)}{\partial t} = [\lambda_a(V,U,t) + \lambda_b(V,U,t)]\delta_{j0} - \left[\frac{\gamma_a - \gamma_{ab} + \gamma_b}{2} + (2j)i\gamma V\right]M_{2j}(V,U,t) - \frac{\gamma_a - \gamma_{ab} - \gamma_b}{2}D_{2j}(V,U,t), \tag{28}$$

$$\frac{dA_r(t)}{dt} = -\frac{1}{2t_c}\left[A_r(t) + \delta(y-y_0)A_i(t) - \int_{-\infty}^{\infty}\int_{-\infty}^{\infty}P_{i,1i}(V,U,t)dVdU\right], \tag{29}$$

$$\frac{dA_i(t)}{dt} = -\frac{1}{2t_c}\left[A_i(t) - \delta(y-y_0)A_r(t) + \int_{-\infty}^{\infty}\int_{-\infty}^{\infty}P_{r,1i}(V,U,t)dVdU\right], \tag{30}$$

where the lower limit on the U integration has been extended to $-\infty$.

Equations (25)–(30) allow for the possibility of a distribution of the natural transition center frequencies (U in the normalized units) and the velocities (V in the normalized units). However, the emphasis in this study is on the pulsation data for homogeneously broadened ensembles of atoms or molecules. Thus the polarization and population variables may be regarded as delta functions of U and V and can be replaced by the new variables

$$P_{r,2j+1}(t) = \int_{-\infty}^{\infty}\int_{-\infty}^{\infty}P_{r,2j+1}(V,U,t)dVdU, \tag{31}$$

$$P_{i,2j+1}(t) = \int_{-\infty}^{\infty}\int_{-\infty}^{\infty}P_{i,2j+1}(V,U,t)dVdU, \tag{32}$$

$$D_{2j}(t) = \int_{-\infty}^{\infty}\int_{-\infty}^{\infty}D_{2j}(V,U,t)dVdU, \tag{33}$$

$$M_{2j}(t) = \int_{-\infty}^{\infty}\int_{-\infty}^{\infty}M_{2j}(V,U,t)dVdU, \tag{34}$$

$$\lambda_a(t) = \int_{-\infty}^{\infty}\int_{-\infty}^{\infty}\lambda_a(V,U,t)dVdU, \tag{35}$$

$$\lambda_b(t) = \int_{-\infty}^{\infty}\int_{-\infty}^{\infty}\lambda_b(V,U,t)dVdU. \tag{36}$$

With these variable changes and with U and V set equal to zero, Eqs. (25)–(30) reduce to

$$\frac{\partial P_{r,2j+1}(t)}{\partial t} = -\gamma\{P_{r,2j+1}(t) + yP_{i,2j+1}(t) + iA_i(t) \times [D_{2j}(t) - D_{2j+2}(t)]\}, \tag{37}$$

$$\frac{\partial P_{i,2j+1}(t)}{\partial t} = -\gamma\{P_{i,2j+1}(t) - yP_{r,2j+1}(t) - iA_r(t) \times [D_{2j}(t) - D_{2j+2}(t)]\}, \tag{38}$$

$$\frac{\partial D_{2j}(t)}{\partial t} = [\lambda_a(t) - \lambda_b(t)]\delta_{j0} - \frac{\gamma_a + \gamma_{ab} + \gamma_b}{2}D_{2j}(t) - \frac{\gamma_a + \gamma_{ab} - \gamma_b}{2}M_{2j}(t) - i\gamma_1\{[A_r(t)P_{i,2j-1}(t) - A_i(t)P_{r,2j-1}(t)] - [A_r(t)P_{i,2j+1}(t) - A_i(t)P_{r,2j+1}(t)]\}, \tag{39}$$

$$\frac{\partial M_{2j}(t)}{\partial t} = [\lambda_a(t) + \lambda_b(t)]\delta_{j0} - \frac{\gamma_a - \gamma_{ab} + \gamma_b}{2}M_{2j}(t) - \frac{\gamma_a - \gamma_{ab} - \gamma_b}{2}D_{2j}(t), \tag{40}$$

$$\frac{\partial A_r(t)}{\partial t} = -\frac{1}{2t_c}[A_r(t) + \delta(y-y_0)A_i(t) - P_{i,1i}(t)], \tag{41}$$

$$\frac{\partial A_i(t)}{\partial t} = -\frac{1}{2t_c}[A_i(t) - \delta(y-y_0)A_r(t) + P_{r,1i}(t)]. \tag{42}$$

Before proceeding further, we make one final simplification of the laser model so that it will contain the minimum number of parameters necessary to obtain qualitative agreement between theoretical and experimental results. One significant complication involves the

energy-level model that has been chosen. This model allows for arbitrary decay rates from each laser level and an arbitrary decay rate between the upper and lower laser levels. As was shown previously, if the lower-state decay rate is related to the upper-state rates by $\gamma_b = \gamma_a + \gamma_{ab}$, then the population sum parameter M and its dynamic equation [Eq. (40)] can be ignored from the general set, because Eq. (39) becomes independent of the parameter M_{2j}.[41] This simplification reduces the number of equations involved in the computation, and Eqs. (37)–(42) can be written as

$$\frac{\partial P_{r,2j+1}(t')}{\partial t'} = -\delta\{P_{r,2j+1}(t') + yP_{i,2j+1}(t') + iA_i(t') \times [D_{2j}(t') - D_{2j+2}(t')]\}, \tag{43}$$

$$\frac{\partial P_{i,2j+1}(t')}{\partial t'} = -\delta\{P_{i,2j+1}(t') - yP_{r,2j+1}(t') - iA_r(t') \times [D_{2j}(t') - D_{2j+2}(t')]\}, \tag{44}$$

$$\frac{\partial D_{2j}(t')}{\partial t'} = \frac{\lambda_d(t')}{\gamma_c}\delta_{j0} - \rho\delta D_{2j}(t') - i\rho\delta \times \{[A_r(t')P_{i,2j-1}(t') - A_i(t')P_{r,2j-1}(t')] - [A_r(t')P_{i,2j+1}(t') - A_i(t')P_{r,2j+1}(t')]\}, \tag{45}$$

$$\frac{dA_r(t')}{\partial t'} = -[A_r(t') + \delta(y - y_0)A_i(t') - P_{i,1i}(t')], \tag{46}$$

$$\frac{dA_i(t')}{\partial t'} = -[A_i(t') - \delta(y - y_0)A_r(t') + P_{r,1i}(t')], \tag{47}$$

where the population difference decay rate $\gamma_d = \gamma_b$ has been introduced together with the decay rate ratios $\delta = \gamma/\gamma_c$, $\rho = \gamma_d/\gamma$, the normalized time $t' = \gamma_c t = t/2t_c$, and the normalized pump rate $\lambda_d(t') = \lambda_a(t') - \lambda_b(t')$. From Eqs. (43)–(47) it follows that with steady-state pumping the pump rate can be expressed in terms of the threshold parameter r by using the equation $\lambda_d = r\gamma_d$.

Equations (43)–(47) have been solved by a second-order Runge–Kutta method, and details about the solutions of related equations can be found in Refs. 35 and 41. Our main interest here is in the stability criteria, which show the conditions under which a small perturbation will grow (type 1 instability boundary) and the conditions under which a large-amplitude oscillation will be maintained (type 2 boundary). The actual shape of the pulsation waveforms is not of particular interest in this study. Unfortunately, the equations governing the instability are sufficiently complex that information about the stability boundaries for general conditions of frequency tuning can be obtained only from the direct numerical solutions. The above equations are the simplest possible starting point for a general look at the stability boundaries of a standing-wave homogeneously broadened laser.

3. LINEAR STABILITY ANALYSIS

Although Eqs. (43)–(47) are needed for a general discussion of the laser stability boundaries, special cases may occur in which semianalytic solutions are possible. In particular, for line center tuning it is possible to obtain the type 1 stability boundary from a solution of the linearized laser model. For this purpose it is best not to make the spatial harmonic expansion that was described in Section 2. Therefore our starting point here is again Eqs. (1)–(6). As a first step we will reduce the model to the homogeneous limit by setting $\omega = \omega_0$ and $v = 0$ and by introducing the new set of variables

$$P_r(z,t) = \int_0^\infty \int_{-\infty}^\infty P_r(v,\omega_\alpha,z,t)\mathrm{d}v\mathrm{d}\omega_\alpha, \tag{48}$$

$$P_i(z,t) = \int_0^\infty \int_{-\infty}^\infty P_i(v,\omega_\alpha,z,t)\mathrm{d}v\mathrm{d}\omega_\alpha, \tag{49}$$

$$D(z,t) = \int_0^\infty \int_{-\infty}^\infty D(v,\omega_\alpha,z,t)\mathrm{d}v\mathrm{d}\omega_\alpha, \tag{50}$$

$$M(z,t) = \int_0^\infty \int_{-\infty}^\infty M(v,\omega_\alpha,z,t)\mathrm{d}v\mathrm{d}\omega_\alpha, \tag{51}$$

$$\lambda_a(z,t) = \int_0^\infty \int_{-\infty}^\infty \lambda_a(v,\omega_\alpha,z,t)\mathrm{d}v\mathrm{d}\omega_\alpha, \tag{52}$$

$$\lambda_b(z,t) = \int_0^\infty \int_{-\infty}^\infty \lambda_b(v,\omega_\alpha,z,t)\mathrm{d}v\mathrm{d}\omega_\alpha. \tag{53}$$

As before, we assume a simplified energy-level model ($\gamma_b = \gamma_a + \gamma_{ab} = \gamma_d$); and we also consider that the laser oscillation frequency is at line center ($\omega = \omega_0$) when the empty cavity mode frequency is at line center ($\Omega = \omega_0$). When these substitutions are made, Eqs. (1)–(6) reduce to

$$\frac{\partial P_r(z,t)}{\partial t} = -\gamma P_r(z,t) + \frac{\mu^2}{\hbar}\sin(kz)E_i(t)D(z,t), \tag{54}$$

$$\frac{\partial P_i(z,t)}{\partial t} = -\gamma P_i(z,t) - \frac{\mu^2}{\hbar}\sin(kz)E_r(t)D(z,t), \tag{55}$$

$$\frac{\partial D(z,t)}{\partial t} = \lambda_d(z,t) - \gamma_d D(z,t) + \frac{1}{\hbar}\sin(kz)[E_r(t)P_i(z,t) - E_i(t)P_r(z,t)], \tag{56}$$

$$\frac{dE_r(t)}{dt} = -\frac{E_r(t)}{2t_c} - \frac{\omega_0}{\epsilon_1 L}\int_0^l \sin(kz)P_i(z,t)\mathrm{d}z, \tag{57}$$

$$\frac{dE_i(t)}{dt} = -\frac{E_i(t)}{2t_c} + \frac{\omega_0}{\epsilon_1 L}\int_0^l \sin(kz)P_r(z,t)\mathrm{d}z, \tag{58}$$

where the normalized pump rate difference is $\lambda_d(z,t) = \lambda_a(z,t) - \lambda_b(z,t)$.

From the form of Eqs. (54)–(58) it follows that we can obtain nontrivial solutions if $P_r(z,t)$ and $E_i(t)$ are arbitrarily set equal to zero. For this stability discussion we will also set the pump rate equal to a constant [$\lambda_d(z,t) = \lambda_d$]. When we make these substitutions, Eqs. (54)–(58) reduce to the smaller set

$$\frac{\partial P_r(z,t)}{\partial t} = -\gamma P_r(z,t) + \frac{\mu^2}{\hbar}\sin(kz)E_i(t)D(z,t), \tag{59}$$

$$\frac{\partial D(z,t)}{\partial t} = \lambda_d - \gamma_d D(z,t) + \frac{1}{\hbar}\sin(kz)E_r(t)P_i(z,t), \tag{60}$$

$$\frac{dE_r(t)}{dt} = -\frac{E_r(t)}{2t_c} - \frac{\omega_0}{\epsilon_1 L}\int_0^l \sin(kz)P_i(z,t)\mathrm{d}z. \tag{61}$$

It is convenient to rewrite Eqs. (59)–(61) by using the normalized length $\zeta = kz$ and the new variables

$$A_r(t) = -\frac{\mu}{2\hbar}\left(\frac{1}{\gamma\gamma_d}\right)^{1/2} E_r(t), \tag{62}$$

$$P_i(\zeta, t) = \frac{\omega_0}{\epsilon_1 L}\frac{\mu}{2\hbar}\left(\frac{1}{\gamma\gamma_d}\right)^{1/2}\frac{1}{\gamma_c}\frac{l}{\pi}P_i(z, t), \tag{63}$$

$$D(\zeta, t) = \frac{\mu^2}{\gamma\hbar}\frac{\omega_0}{\epsilon_1 L}\frac{1}{\gamma_c}\frac{l}{2\pi}D(z, t), \tag{64}$$

$$D_0 = \frac{\mu^2}{\gamma\hbar}\frac{\omega_0}{\epsilon_1 L}\frac{1}{\gamma_c}\frac{l}{2\pi}\frac{\lambda_d}{\gamma_d}. \tag{65}$$

With these substitutions, Eqs. (59)–(61) take the form

$$\frac{\partial P_i(\zeta, t)}{\partial t} = -\gamma[P_i(\zeta, t) + 2\sin(\zeta)A_r(t)D(\zeta, t)], \tag{66}$$

$$\frac{\partial D(\zeta, t)}{\partial t} = -\gamma_d[D(\zeta, t) - D_0 - 2\sin(\zeta)A_r(t)P_i(\zeta, t)], \tag{67}$$

$$\frac{\partial A_r(t)}{\partial t} = -\gamma_c[A_r(t) + 2\int_0^{\pi/2}\sin(\zeta)P_i(\zeta, t)\mathrm{d}\zeta]. \tag{68}$$

Equations (66)–(68) form the basis for our linear stability analysis of a homogeneously broadened standing-wave laser. As a first step, the steady-state solution of these equations must be obtained. From Eqs. (66) and (67) we find that the steady-state values of the polarization and population difference are given by

$$P_{is}(\zeta) = -2\sin(\zeta)A_{rs}D_s(\zeta), \tag{69}$$

$$D_s(\zeta) = \frac{D_0}{1 + 4\,sin^2(\zeta)\mathrm{A_{rs}}^2}. \tag{70}$$

With these results, the steady-state field is obtained from Eq. (68) as

$$1 = 4\int_0^{\pi/2}\frac{\sin^2(\zeta)D_0}{1 + 4\sin^2(\zeta)A_{rs}^2}\mathrm{d}\zeta. \tag{71}$$

At threshold the field A_{rs} vanishes, and Eq. (71) reduces to

$$1 = 4\int_0^{\pi/2}\sin^2(\zeta)D_0\mathrm{d}\zeta = \pi D_0. \tag{72}$$

Therefore it is convenient to introduce the threshold parameter $r = \pi D_0$, and one can integrate Eq. (71) to obtain

$$\begin{aligned} 1 &= \frac{4r}{\pi}\int_0^{\pi/2}\frac{\sin^2(\zeta)}{1 + 4\sin^2(\zeta)A_{rs}^2}\mathrm{d}\zeta \\ &= \frac{2r}{\pi}\int_0^{\pi/2}\frac{1 - \cos(2\zeta)}{1 + 4\sin^2(\zeta)A_{rs}^2}\mathrm{d}\zeta \\ &= \frac{2r}{1 + 4A_{rs}^2 + (1 + 4A_{rs}^2)^{1/2}}, \end{aligned} \tag{73}$$

where we have used the equation[42]

$$\int_0^{\pi/2}\frac{\cos(2nx)}{1 - a^2\sin^2(x)}\mathrm{d}x = \frac{(-1)^n\pi}{2(1 - a^2)^{1/2}}\left(\frac{1 - (1 - a^2)^{1/2}}{a}\right)^{2n}. \tag{74}$$

Equation (73) is a quadratic equation for the parameter $(1 + 4A_{rs})^{1/2}$, and the useful solution is

$$(1 + 4A_{rs}^2)^{1/2} = \frac{-1 + (1 + 8r)^{1/2}}{2}. \tag{75}$$

From this equation, one can solve for the intensity $I = A_{rs}^2$, and the result is[43]

$$A_{rs}^2 = \frac{4r - 1 - (1 + 8r)^{1/2}}{8}. \tag{76}$$

The next step in this linear stability analysis is to represent the dependent variables in terms of perturbations of the steady-state solutions that have just been obtained. Thus the polarization, the population difference, and the field are now written as

$$P_i(\zeta, t) = P_{is}(\zeta) + P_i'(\zeta, t), \tag{77}$$

$$D(\zeta, t) = D_s(\zeta) + D'(\zeta, t), \tag{78}$$

$$A_r(t) = A_{rs} + A_r'(t), \tag{79}$$

where the subscript s indicates the steady-state solutions and the primed quantities represent the small perturbations of the corresponding parameters. Substituting these linearized parameters into Eqs. (66)–(68) and neglecting second-order terms in the small quantities, one can reduce the equations to

$$\begin{aligned} \frac{\mathrm{d}P_i'(\zeta, t)}{\mathrm{d}t} &= -\gamma\{P_i'(\zeta, t) + 2\sin(\zeta) \\ &\quad \times [A_{rs}D'(\zeta, t) + A_r'(t)D_s(\zeta)]\}, \end{aligned} \tag{80}$$

$$\begin{aligned} \frac{\mathrm{d}D'(\zeta, t)}{\mathrm{d}t} &= -\gamma_d\{D'(\zeta, t) - 2\sin(\zeta) \\ &\quad \times [A_{rs}P_i'(\zeta, t) + A_r'(t)P_{is}(\zeta)]\}, \end{aligned} \tag{81}$$

$$\frac{\mathrm{d}A_r'(t)}{\mathrm{d}t} = -\gamma_c[A_r'(t) + 2\int_0^{\pi/2}\sin(\zeta)P_i'(\zeta, t)\mathrm{d}\zeta]. \tag{82}$$

Equations (80)–(82) are a linear first-order set, and the solutions can be written in the exponential forms

$$P_i'(\zeta, t) = P_i''(\zeta)\exp(st), \tag{83}$$

$$D'(\zeta, t) = D''(\zeta)\exp(st), \tag{84}$$

$$A_r'(t) = A_r''\exp(st), \tag{85}$$

where s is a complex rate constant. With these substitutions, Eqs. (80)–(82) reduce to

$$sP_i''(\zeta) = -\gamma\{P_i''(\zeta) + 2\sin(\zeta)[A_{rs}D''(\zeta) + A_r''D_s(\zeta)]\}, \tag{86}$$

$$sD''(\zeta) = -\gamma_d\{D''(\zeta) - 2\sin(\zeta)[A_{rs}P_i''(\zeta) + A_r''P_{is}(\zeta)]\}, \tag{87}$$

$$sA_r'' = -\gamma_c\left[A_r'' + 2\int_0^{\pi/2}\sin(\zeta)P_i''(\zeta)\mathrm{d}\zeta\right]. \tag{88}$$

Equations (86)–(88) may be solved separately for the dependent variables appearing on the left-hand sides of the

equations, and the results are

$$P_i''(\zeta) = -\frac{2\gamma \sin(\zeta)}{s+\gamma}\left[\frac{A_r''r/\pi}{1+4\sin^2(\zeta)A_{rs}^2} + A_{rs}D''(\zeta)\right], \tag{89}$$

$$D''(\zeta) = \frac{2\gamma_d \sin(\zeta)}{s+\gamma_d}\left[-\frac{2\sin(\zeta)A_{rs}A_r''r/\pi}{1+4\sin^2(\zeta)A_{rs}^2} + A_{rs}P_i''(\zeta)\right], \tag{90}$$

$$A_r'' = -\frac{2\gamma_c}{s+\gamma_c}\int_0^{\pi/2}\sin(\zeta)P_i''(\zeta)\mathrm{d}\zeta, \tag{91}$$

where Eqs. (69) and (70) have been substituted for the P_{is} and D_s terms. Equation (90) may be used to eliminate $D''(\zeta)$ from Eq. (89), and the result can be written as

$$P_i''(\zeta) = -\frac{\left\{\frac{2\gamma \sin(\zeta)A_r''r/\pi}{(s+\gamma)[1+4\sin^2(\zeta)A_{rs}^2]}\right\}\left[1-\frac{4\gamma_d \sin^2(\zeta)A_{rs}^2}{s+\gamma_d}\right]}{1+\frac{4\gamma\gamma_d \sin^2(\zeta)A_{rs}^2}{(s+\gamma)(s+\gamma_d)}}. \tag{92}$$

When this value of $P_i''(\zeta)$ is substituted into Eq. (91), one obtains the following equation for the complex rate constant s:

$$1 = \frac{4\gamma\gamma_c r/\pi}{(s+\gamma)(s+\gamma_c)} \times \int_0^{\pi/2}\frac{\sin^2(\zeta)\left[1-\frac{4\gamma_d \sin^2(\zeta)A_{rs}^2}{s+\gamma_d}\right]}{[1+4\sin^2(\zeta)A_{rs}^2]\left[1+\frac{4\gamma\gamma_d \sin^2(\zeta)A_{rs}^2}{(s+\gamma)(s+\gamma_d)}\right]}\mathrm{d}\zeta. \tag{93}$$

The integrals implicit in Eq. (93) can be simplified by partial fraction expansions, and the resulting integrations may be performed by using Eq. (74). In this way we have obtained the result

$$1 = \frac{2\gamma\gamma_c r/[(s+\gamma)(s+\gamma_c)]}{4\gamma\gamma_d A_{rs}^2/[(s+\gamma)(s+\gamma_d)] - 4A_{rs}^2} \times \left(\left\{\frac{1}{(1+4A_{rs}^2)^{1/2}} - \frac{1}{\left[1+\frac{4\gamma\gamma_d A_{rs}^2}{(s+\gamma)(s+\gamma_d)}\right]^{1/2}}\right\} - \frac{4\gamma_d A_{rs}^2}{s+\gamma_d}\left\{\frac{1}{1+4A_{rs}^2+(1+4A_{rs}^2)^{1/2}} - \frac{1}{1+\frac{4\gamma\gamma_d A_{rs}^2}{(s+\gamma)(s+\gamma_d)}+\left[1+\frac{4\gamma\gamma_d A_{rs}^2}{(s+\gamma)(s+\gamma_d)}\right]^{1/2}}\right\}\right). \tag{94}$$

Equation (94) is probably not solvable by analytical methods, but numerical solutions are always possible. It is helpful to first reduce the number of variables appearing in this equation by substituting $\delta = \gamma/\gamma_c$ and $\rho = \gamma_d/\gamma$, which were introduced in Section 2. Then Eq. (94) has the form

$$1 = \frac{\frac{2\delta r}{(s'+1)(s'+\delta)}}{\frac{4\delta^2\rho A_{rs}^2}{(s'+\delta)(s'+\delta\rho)} - 4A_{rs}^2} \times \left(\left\{\frac{1}{(1+4A_{rs}^2)^{1/2}} - \frac{1}{\left[1+\frac{4\delta^2\rho A_{rs}^2}{(s'+\delta)(s'+\delta\rho)}\right]^{1/2}}\right\} - \frac{4\delta\rho A_{rs}^2}{s'+\delta\rho}\left\{\frac{1}{1+4A_{rs}^2+(1+4A_{rs}^2)^{1/2}} - \frac{1}{1+\frac{4\delta^2\rho A_{rs}^2}{(s'+\delta)(s'+\delta\rho)}+\left[1+\frac{4\delta^2\rho A_{rs}^2}{(s'+\delta)(s'+\delta\rho)}\right]^{1/2}}\right\}\right), \tag{95}$$

where the new complex rate constant $s' = s/\gamma_c$ has also been introduced.

It is possible by means of algebraic manipulations to clear the radicals from Eq. (95), and the result can be expressed in the form of a polynomial in the parameter s'. Numerical methods have been used to obtain the roots of this polynomial. Not all these roots are meaningful, however, because the process of transforming the radical equation into the polynomial equation introduces spurious roots. The spurious roots can be identified by substitution of the solutions back into the radical equation. All the solutions we have obtained have been checked by this method.

4. RESULTS

For the studies of interest here, the results consist of curves in laser parameter space separating the regions in which the laser output is continuous wave from the regions in which undamped output pulsations occur. As we have already noted, two distinguishable types of instability boundary are seen. The first type (type 1) identifies the regions where infinitesimal perturbations from steady state will grow into large-amplitude pulsations, and the second type (type 2) identifies the regions where large-amplitude oscillations will be sustained. The perturbation stability boundaries can be obtained in two different ways in our analysis. For line center tuning it is possible to use the semianalytical method described in Section 3. Thus, for a given set of laser parameters, we have obtained the roots of the polynomial equation discussed above and eliminated spurious roots by checking against Eq. (95). We have then checked to see whether any of the remaining roots has positive real parts, as the existence of such parts indicates that the steady-state solution is unstable with respect to small perturbations. To verify our analytical and numerical methods, we have also compared some of our semianalytical solutions with the numerical results obtained by direct integration of Eqs. (43)–(47). We have usually used 20 or more spatial harmonics in the numerical solutions; for the parameter range that we have studied, good convergence of the numerical solutions has been obtained.

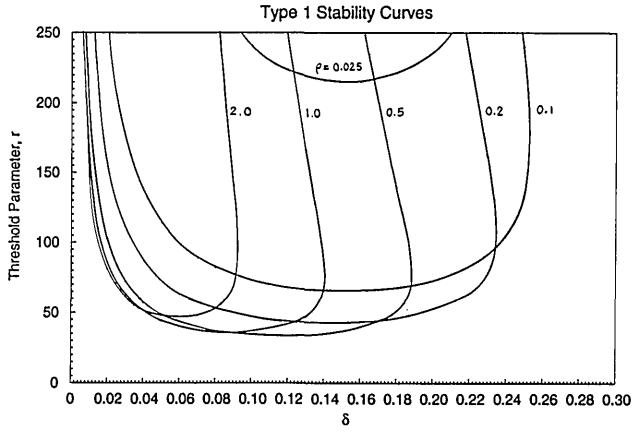

Fig. 1. Type 1 (perturbation) stability criteria for a line center tuned homogeneously broadened standing-wave oscillator for various values of the decay rate ratios $\delta = \gamma/\gamma_c$ and $\rho = \gamma_d/\gamma_0$. Above or inside one of these curves an infinitesimal perturbation will exhibit oscillatory growth with time, while outside or below a curve the perturbation will decay away.

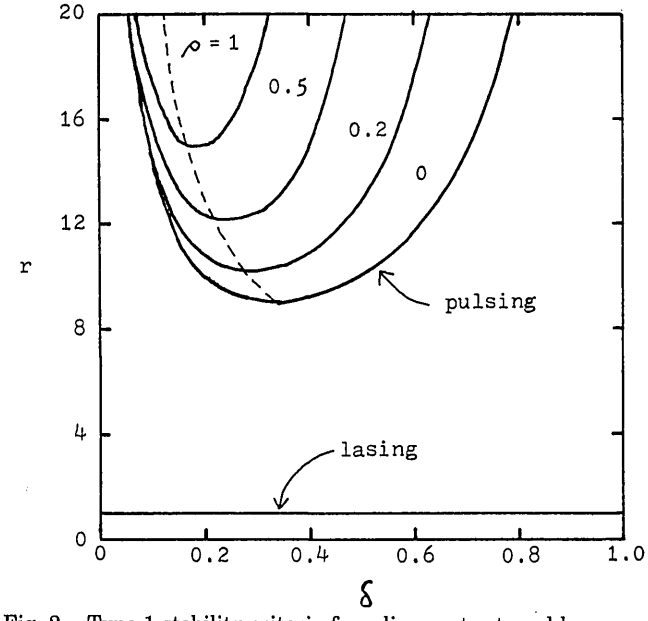

Fig. 2. Type 1 stability criteria for a line center tuned homogeneously broadened ring-laser oscillator (after Ref. 34).

The results for the type 1 perturbation stability boundary are shown in Fig. 1 for a range of values of the parameters δ, ρ, and r. The threshold at which a laser starts lasing corresponds to when the threshold parameter r is equal to one. Above each curve is where the real part of at least one of the solutions for the normalized complex rate constant is positive. Thus, in this region a small perturbation will grow with time, and operation is unstable. Below each curve, on the other hand, the real part of each of the values of the normalized rate constant is negative, and a small perturbation will decay with time. Thus, operation in that region is stable with respect to small perturbations.

One of the most interesting results shown by Fig. 1 is that the value of the threshold parameter required to reach the unstable region is very high. The minimum value shown in the figure is approximately 34 times above the lasing threshold. This result may be compared with the corresponding stability criteria for ring lasers, shown in Fig. 2, where the lowest value of the perturbation stability boundary is nine times above the lasing threshold.[34] Thus there appears to be a greater possibility that we might observe spontaneous coherent pulsation behavior in a ring laser than in a standing-wave laser. It is, of course, still necessary to check the type 2 instability boundary to verify that large-amplitude oscillations are also not possible for more-modest values of the threshold parameter.

A set of curves representing the type 2 stability boundaries is shown in Fig. 3. These results show the minimum values of the threshold parameter for which large-amplitude oscillations will not decay with time. This threshold condition corresponds to a laser that pulses initially. The threshold parameter is then gradually reduced until the pulsations stop. We can see that there is little difference between the two types of stability criteria shown in Figs. 1 and 3. The minimum value of the

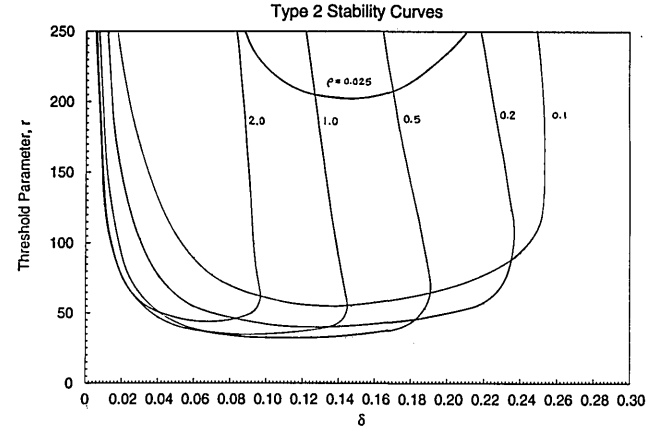

Fig. 3. Type 2 (large-amplitude) stability criteria for a line center tuned homogeneously broadened standing-wave laser oscillator. Above or inside one of these curves a large-amplitude oscillation can exist indefinitely, while outside or below a curve the oscillation will decay.

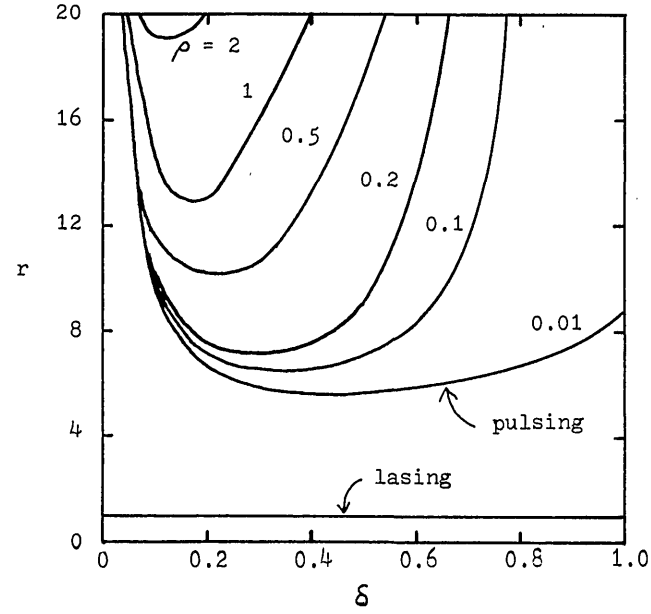

Fig. 4. Type 2 stability criteria for a line center tuned homogeneously broadened ring laser oscillator (after Ref. 34).

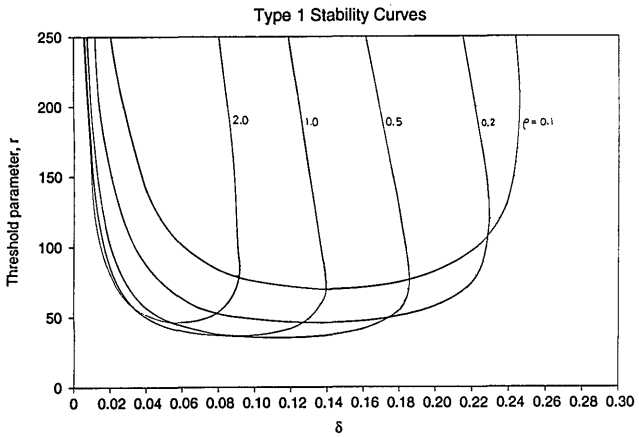

Fig. 5. Type 1 stability criteria for a standing-wave homogeneously broadened laser oscillator that is detuned by 0.5 $\Delta\nu_h$.

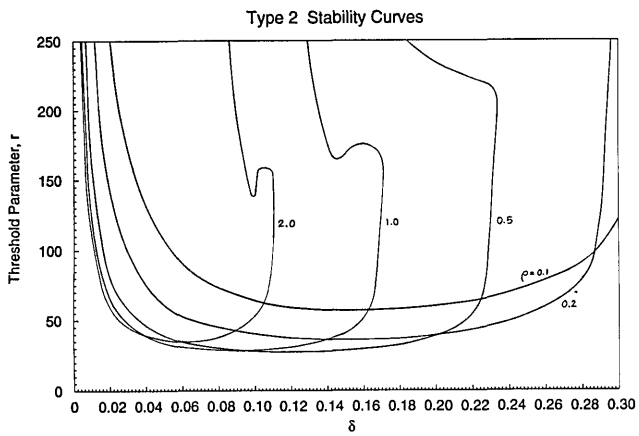

Fig. 6. Type 2 stability criteria for a standing-wave homogeneously broadened laser oscillator that is detuned by 0.5 $\Delta\nu_h$.

threshold parameter in Fig. 3 is approximately 33 times above the lasing threshold. It is clear that the pulsation behavior in single-mode homogeneously broadened standing-wave lasers would be extremely difficult to observe. The large value of the threshold parameter must be achieved at the same time that the laser is operating with the high cavity losses necessary to satisfy the condition that δ be well below unity. For comparison, the type 2 stability threshold for a homogeneously broadened ring laser is shown in Fig. 4, and the lowest value is only approximately $r = 5$.[34] Note that pulsations in the ring laser are possible for values of δ greater than unity.[34,36,37]

The stability criteria of both type 1 and type 2 for detuned lasers are shown in Figs. 5 and 6. We have chosen for these examples the detuning value of half the homogeneous linewidth ($\Delta\nu = \Delta\nu_h/2$). With this detuning, the value of the threshold parameter needed to initiate lasing is equal to two, which means that a laser needs to be pumped twice as hard as for line center operation. From the figures one can observe that the effect of detuning is to raise the type 1 stability boundary and to decrease the type 2 boundary. A similar effect was also reported for the ring-laser model.[37] Thus it should be slightly easier (but still difficult) to maintain large-amplitude spontaneous pulsations in a detuned homogeneously broadened standing-wave laser.

5. DISCUSSION

In this study we have developed stability criteria for strongly homogeneously broadened standing-wave laser oscillators. The results show a significant difference between the stability criteria for standing-wave laser oscillators and the criteria for ring-laser oscillators. In the case of line center tuning, we find from the type 1 criterion that undamped pulsations in strongly homogeneously broadened standing-wave laser oscillators occur at a much higher minimum excitation level (~34) than in ring-laser oscillators (9). In contrast to ring lasers, standing-wave lasers seem always to require the condition $\delta < 1$. We found that detuning tends to raise the type 1 instability threshold and decrease the type 2 instability threshold, as observed previously in ring-laser oscillators. Thus detuning leads to a wider marginal oscillation area.

Until now, there have been no reports of the successful experimental observation of instabilities in homogeneously broadened standing-wave laser oscillators. In some far-infrared laser experiments, however, the ring cavity required for unidirectional traveling-wave operation was replaced by a standing-wave cavity.[16,17] In these cases the laser material was Doppler broadened, but the optical signal was tuned away from line center so that the individual molecules still interacted with only one of the traveling-wave components of the standing-wave field. To observe true standing-wave instabilities in homogeneously broadened lasers, one would need to use lasers having high levels of gain and narrow homogeneous linewidths. The best prospects would probably involve standing-wave modifications of the far-infrared ring-laser systems that have already been studied thoroughly. The effects of inhomogeneous broadening on the stability criteria for standing-wave lasers are also of interest, and we hope to report on that subject soon. Inhomogeneously broadened lasers exhibit a low threshold spontaneous pulsation instability for both ring and standing-wave configurations, and the experimental results have been well described by theoretical models.

ACKNOWLEDGMENTS

This research was supported in part by the National Science Foundation and by Tektronix, Inc.

REFERENCES AND NOTES

1. L. W. Casperson, "Spontaneous pulsations in lasers," in *Third New Zealand Symposium on Laser Physics*, J. D. Harvey and D. F. Walls, eds., Vol. 182 of Springer Lecture Notes in Physics (Springer-Verlag, Berlin, 1983), pp. 88–106.
2. J. C. Englund, R. R. Snapp, and W. C. Schieve, "Fluctuations, instabilities and chaos in the laser driven nonlinear ring cavity," Prog. Opt. **21,** 355–428 (1984).
3. J. R. Ackerhalt, P. W. Milonni, and M.-L. Shih, "Chaos in quantum optics," Phys. Rep. **128,** 205–300 (1985).
4. R. G. Harrison and D. J. Biswas, "Pulsating instabilities and chaos in lasers," Prog. Quantum Electron. **10,** 147–228 (1985).
5. W. J. Firth, "Instabilities and chaos in lasers and optical resonators," in *Chaos*, A. V. Holden, ed. (Princeton U. Press, Princeton, N.J., 1986), pp. 135–157.
6. N. B. Abraham, P. Mandel, and L. M. Narducci, "Dynamical instabilities and pulsations in lasers," Prog. Opt. **25,** 1–190 (1988).

7. C. O. Weiss, "Chaotic laser dynamics," Opt. Quantum Electron. **20,** 1–22 (1988).
8. P. W. Milonni, M.-L. Shih, and J. R. Ackerhalt, *Chaos in Laser Matter Interactions* (World Scientific, Singapore, 1987).
9. E. N. Lorenz, "Deterministic non-periodic flows," J. Atmos. Sci. **20,** 130–141 (1963).
10. H. Haken, "Analogy between higher instabilities in fluids and lasers," Phys. Lett. **53A,** 77–78 (1975).
11. C. O. Weiss and W. Klische, "On observability of Lorenz instabilities in lasers," Opt. Commun. **51,** 47–48 (1984).
12. C. O. Weiss, "Observation of instabilities and chaos in optically pumped far-infrared lasers," J. Opt. Soc. Am. B **2,** 137–140 (1985).
13. C. O. Weiss, W. Klische, P. S. Ering, and M. Cooper, "Instabilities and chaos of a single-mode NH_3 ring laser," Opt. Commun. **52,** 405–408 (1985).
14. W. Klische and C. O. Weiss, "Instabilities and routes to chaos in a homogeneously broadened one- and two-mode ring laser," Phys. Rev. A **31,** 4049–4051 (1985).
15. C. O. Weiss and J. Brock, "Evidence of Lorenz-type chaos in a laser," Phys. Rev. Lett. **57,** 2804–2806 (1986).
16. E. H. M. Hogenboom, W. Klische, C. O. Weiss, and A. Godone, "Instabilities of a homogeneously broadened laser," Phys. Rev. Lett. **55,** 2571–2574 (1985).
17. N. B. Abraham, D. Dangoisse, P. Glorieux, and P. Mandel, "Observation of undamped pulsations in a low-pressure, far-infrared laser and comparison with a simple theoretical model," J. Opt. Soc. Am. B **2,** 23–24 (1985).
18. M. Y. Li, T. Win, C. O. Weiss, and N. R. Heckenberg, "Attractor properties of laser dynamics: a comparison of NH_3-laser emission with the Lorenz model," Opt. Commun. **80,** 119–126 (1990).
19. D. Y. Tang, C. O. Weiss, E. Roldan, and G. J. de Valcarcel, "Deviation from Lorenz-type dynamics of an NH_3 ring laser," Opt. Commun. **89,** 47–53 (1992).
20. L. W. Casperson and A. Yariv, "The time behavior and spectra of relaxation oscillations in a high gain laser," IEEE J. Quantum Electron. **QE-8,** 69–73 (1972).
21. L. W. Casperson, "Spontaneous coherent pulsations in laser oscillators," IEEE J. Quantum Electron. **QE-14,** 756–761 (1978).
22. M. A. Dupertuis, R. R. E. Salomaa, and M. R. Siegrist, "The conditions for Lorenz chaos in an optically-pumped far-infrared laser," Opt. Commun. **57,** 410–414 (1986).
23. R. Corbalan, F. Laguarta, J. Pujol, and R. Vilaseca, "Lorenz-like dynamics in Doppler broadened coherently pumped lasers," Opt. Commun. **71,** 290–294 (1989).
24. U. Hubner, N. B. Abraham, and C. O. Weiss, "Dimensions and entropies of chaotic intensity pulsations in a single-mode far-infrared NH_3 laser," Phys. Rev. A **40,** 6354–6365 (1989).
25. C. O. Weiss, N. B. Abraham, and U. Hubner, "Homoclinic and heteroclinic chaos in a single-mode laser," Phys. Rev. Lett. **61,** 1587–1590 (1988).
26. N. B. Abraham and C. O. Weiss, "Dynamical frequency shifts and intensity pulsations in a FIR bidirectional ring laser," Opt. Commun. **68,** 437–441 (1988).
27. C. O. Weiss and N. B. Abraham, "Characterizing chaotic attractors underlying single mode laser emission by quantitative laser field and phase measurement," in *Measures of Complexity and Chaos,* B. Abraham, Al. M. Albano, A. Passamante, and P. E. Rapp, eds. (Plenum, New York, 1989), pp. 269–280.
28. E. Roldan, G. J. de Valcarcel, R. Vilaseca, F. Silba, J. Pujol, R. Corbalan, and F. Laguarta, "Phase dynamics in a Doppler broadened optically-pumped laser," Opt. Commun. **73,** 506–510 (1989).
29. C. O. Weiss, W. Klische, N. B. Abraham, and U. Hubner, "Comparison of NH_3 laser dynamics with the extended Lorenz model," Appl. Phys. B **49,** 211–215 (1989).
30. D. Y. Tang, M. Y. Li, and C. O. Weiss, "Field dynamics of a single-mode laser," Phys. Rev. A **44,** 7597–7604 (1991).
31. H. Zeghlache and P. Mandel, "Phase and amplitude dynamics in the laser Lorenz model," Phys. Rev. A **38,** 3128–3131 (1988).
32. R. Vilaseca, G. J. de Valcarcel, and E. Roldan, "Physical interpretation of laser phase dynamics," Phys. Rev. A **41,** 5269–5272 (1991).
33. G. J. de Valcarcel, E. Roldan, and R. Vilaseca, "Lorenz character of the Doppler-broadened far-infrared laser," J. Opt. Soc. Am. B **8,** 2420–2428 (1991).
34. L. W. Casperson, "Spontaneous coherent pulsations in ring-laser oscillators: stability criteria," J. Opt. Soc. Am. B **2,** 993–997 (1985).
35. L. W. Casperson, "spontaneous coherent pulsations in standing-wave laser oscillators," J. Opt. Soc. Am. B **5,** 958–969 (1988).
36. L. W. Casperson, "Stability criteria for lasers with mixed line broadening," Opt. Quantum Electron. **19,** 29–36 (1987).
37. L. W. Casperson, "Recent progress in modeling single-mode laser instabilities," in *Optical Instabilities,* R. W. Boyd, M. G. Raymer, and L. M. Narducci, eds., Vol. 4 of Cambridge Studies in Modern Optics (Cambridge U. Press, Cambridge, 1986), pp. 58–71.
38. W. E. Lamb, Jr., "Theory of an optical maser," Phys. Rev. **134,** A1429–A1450 (1964).
39. L. A. Lugiato and L. M. Narducci, "Nonlinear dynamics in a Fabry–Perot resonator," Z. Phys. B **71,** 129–138 (1988).
40. Ref. 35, Eqs. (15)–(20).
41. L. W. Casperson and M. F. H. Tarroja, "Spontaneous coherent pulsations in standing-wave laser oscillators: simplified models," J. Opt. Soc. Am. B **8,** 250–261 (1991).
42. I. S. Gradshteyn and I. M. Ryzhik, *Table of Integrals, Series, and Products* (Academic, New York, 1979), Eq. (3.165.1), p. 368.
43. L. W. Casperson, "Laser power calculations: sources of error," Appl. Opt. **19,** 422–434 (1980), Eq. (38).